Viareggio
19 November 2012

## Introduction

In recent years CAEN has developed a complete family of digitizers that consists of several models differing in sampling frequency, resolution, form factor and other features. Besides the use of the digitizers as waveform recorders (oscilloscope mode), CAEN offers the possibility to upload special versions of the FPGA firmware that implement algorithms for the Digital Pulse Processing (DPP); when the digitizer runs in DPP mode, it becomes a new instrument that represents a complete digital replacement of most traditional modules such as Multi Channel Analyzers, QDCs, TDCs, Discriminators and many others. In this application note, we describe the capability of the series x720 (12 bit, 250MSps) to perform neutron-gamma discrimination based upon the digital pulse shape analysis. The development of this FPGA firmware was based upon liquid scintillating detectors of type BC501-A.

All detector and neutron/gamma source based tests were performed at the Triangle Universities Nuclear Laboratory (TUNL) on the campus of the Duke University in collaboration with Mohammad Ahmed.

### Neutron-Gamma discrimination with liquid scintillators

Liquid scintillating detectors are widely used to achieve neutron-gamma discrimination due to their effective Pulse Shape Discrimination (PSD) properties [1].

The light emission of liquid scintillating detectors comprises of a fast decay component, as well as a substantial slow decay component. These components arise from de-excitations of different atomic states in the scintillator. The relative population of these states depends on the energy loss (dE/dx) of the particle. In organic liquid scintillators, these components strongly depend on the energy loss.

The gamma rays interact in the scintillator mostly via atomic Compton scattering or pair production mechanisms. The neutrons are detected by scattering them with the protons. These two different processes for gamma-rays and neutrons give rise to significant difference in the slow decay component of the light emission. This difference becomes the basis of pulse shape discrimination in the liquid scintillating detectors [2].
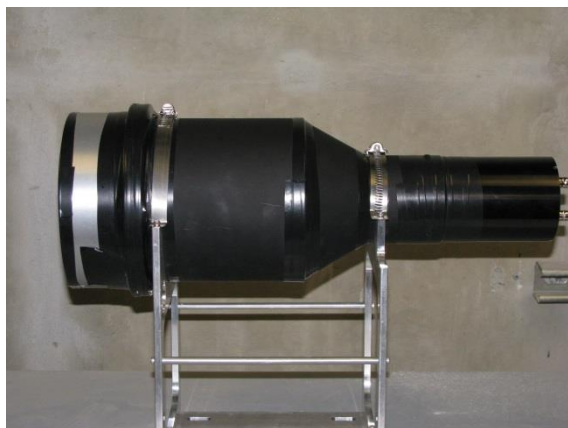
### Set-up description



**Fig. 1: The detector used for these measures is a 5"x2" BC501-A liquid scintillator coupled to an Hamamatsu R1250 PMT**

The detector is a 5 inch diameter, 2 inch thick liquid scintillator of type BC501-A. The scintillator is coupled to a Hamamatsu R1250 photo-multiplier tube (PMT). The base is also a Hamamatsu model HTV H6527. The detector is biased to -1430V.

The signals from the PMTs are connected to the digitizer inputs via 120 feet low-loss RG8 cables.

The detector is biased to -1430V. The signals from the PMTs are connected to the digitizer inputs via 120 feet low-loss RG8 cables.

The digitizer is a 4 channel, 12 bit, 250 MS/s DT5720 (Desktop version). The analog bandwidth is about 120 MHz and the input dynamic range is 2 Vpp; the DC offset can be adjusted by means of an internal DAC in the range -2/+2 V.

The digitizer runs the preliminary version of the DPP-PSD firmware for the digital charge integration and neutron-gamma discrimination. This principle of operation of the DPP-PSD firmware can be summarized by the following operations that are executed in real time inside the FPGA

- The baseline of the signal is calculated by a programmable length mean filter and subtracted from the input signal; the result is compared with the trigger threshold and, if exceeded, a trigger is issued; it is also possible to use the threshold only to get armed, then wait for the pulse peak and issue the trigger at that time.

- With the trigger, the baseline is frozen, two gates of programmable width are opened and the charge integration starts; the signal fed to the integrator is delayed of a programmable number of samples in order to let the gates to start before the trigger.

- The trigger also initiates the event building: this can include the waveforms (i.e. row samples) of the input, baseline, trigger, gate and other signals, the time stamp of the trigger and the charges calculated within the two gates (short and long).

- At the end of the long gate, the baseline calculation restarts and the system gets ready for a new event; if the waveform mode is enabled, the recording continues until the requested number of samples have been saved into the memory.

With the DPP-PSD firmware, each channel has the ability to detect the input pulses and to self trigger independently by the other channels. Common triggering is still possible using the external or software trigger.

**Fig. 2: Digitizer Mod. DT5720 (4 channel, 12 bit, 250MS/s) used for this test**

### *Calibration*

The energy calibration of the liquid scintillating detector was performed using the 662 keV gamma-ray from a $^{137}$Cs source. The Compton scattered gamma rays produce a "Compton Edge". Due to multiple scattering effects, the hard Compton edge is smeared towards higher energies to produce the spectrum as shown in Fig. 1.2 in which the peak is clearly recognizable.

Compton edge can be determined [3] using:

$$N_c = N_P + 1.177\sigma$$

$N_c$ = channel number of the Compton edge

$N_P$ = channel number of the edge peak centroid

$\sigma$ = standard deviation of the edge peak

The spot half-way from the maximum is taken as the "1-Cs-Edge" and the thresholds are set with respect to this Cs-Edge. For example, in the Fig 1.2 the 1-Cs-Edge is about 3750 ADC channels, a 1/8 Cs threshold would be at 468 ADC channels.
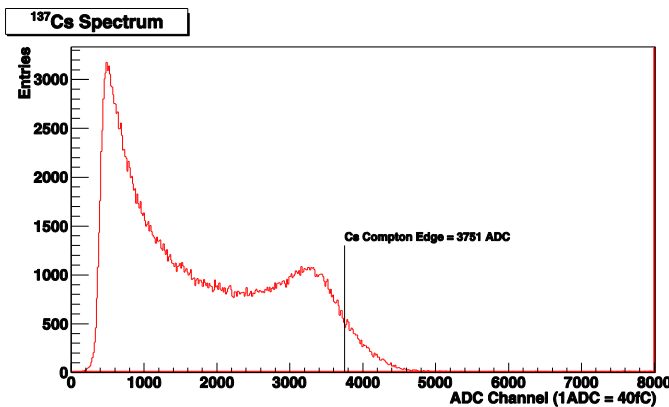


**Fig. 3: Cs-137 Spectrum with the Compton edge at 447 keV used for the calibration**

## Neutron - Gamma Measurements

We used an Americium-Beryllium (AmBe) source placed at about 1 meter away from the detector (measured rate = 2 kcounts/s) as a source of neutrons and gamma rays. The DPP-PSD parameters used for the acquisition are reported in Tab. 1. It is worth noticing that the value of the trigger threshold is not equal to the energy threshold, although they are somehow related. In fact, the trigger threshold is actually the voltage (in ADC counts) that a pulse must exceed in order to be triggered. Instead, the energy is represented by the charge accumulated within the long gate.

| | | |
|---|---|---|
| TRIGGER THRESHOLD | 100 | 1 ADC count = 0.5mV |
| SHORT GATE WIDTH | 100 ns | = 25 samples |
| LONG GATE WIDTH | 320 ns | = 80 samples |
| GATE ANTICIPATION | 40 ns | This is the delay applied to the input signal before entering the accumulator; it defines how long the gates start be |
| BASELINE THRESHOLD | 3 | This threshold is used to exclude noise spikes from the baseline calculation |
| NUM SAMP BL | 16 | Number of samples for the calculation of the baseline (mean filter) |
| SENSITIVITY | 40fC/LSB | This parameter defines the sensitivity of the charge integrator and it determines the full scale range of the charge (which is expressed as a 16 bit number) |

**Tab. 1: DPP-PSD parameters**

In Fig. 4 the average waveforms of neutron and gamma particles are shown. These waveforms are realized averaging off-line 50 events per particle characterized by the same area. It is possible to notice the higher fraction of slow component for neutrons than gammas. The short and the long gate used in the acquisition are also shown.
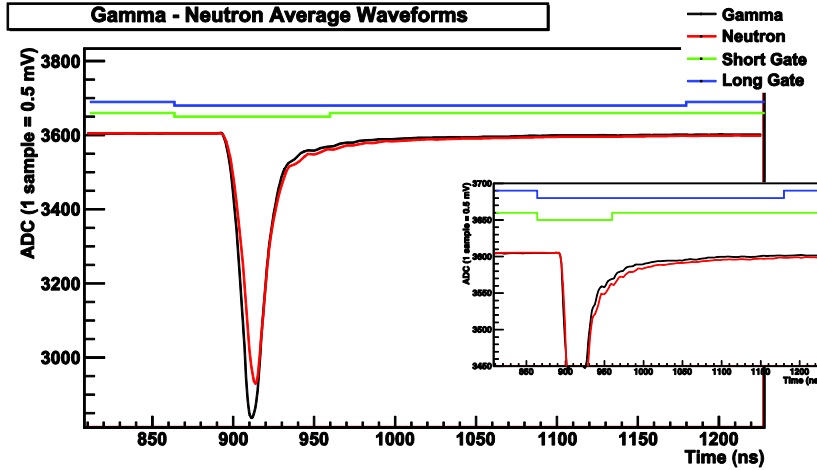


Fig. 4: Average waveforms of neutron and gamma pulses. In the right corner, a zoom showing the different fraction of slow component for gammas and neutrons is drawn.on

The PSD (pulse shape discrimination) is a number that is calculated (off line) according to the following formula:

$$PSD = \frac{Q_L - Q_S}{Q_L}$$

$Q_L$ = charges calculated within long gate
$Q_S$ = charges calculated within short gate

During the acquisition, the list of the events (Time Stamp + QS + QL) is read from the DT5720 and saved to disk (one file per channel). At the end of the acquisition, the files are post processed in order to calculate the energy histograms, the PSD number and to make the relevant plots. We are here considering a run of 200000 events.

Fig. 2.2 is a 2D plot of the counts as function of the pulse Energy (X-axis) and PSD (Y-axis); the two lobes of the neutrons and gammas are well separated and they don't present any bending, thus making easy the n-g discrimination.
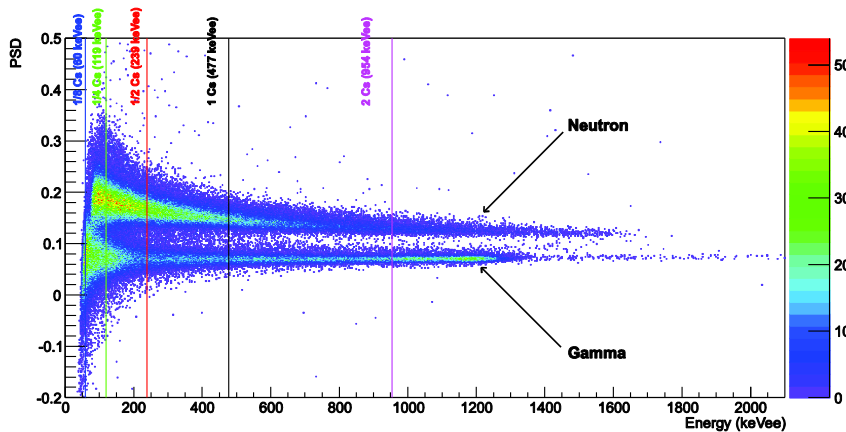


Fig. 5: 2D plot of Energy versus PSD (AmBe source @ 2 kcounts/s)

To quantify the separation of the lobes, it is possible to make an energy cut, take only the points of the 2D plot above that energy and project them along the Y-axis. The resulting plot has the PSD on the X axis and the counts on the Y axis. The energy cut is applied off-line.

In Fig. 6 such a plot is shown for five different energy cuts, that is 1/8, 1/4, 1/2, 1 and 2 times the 137Cs- Compton edge. Note that 1/8 is about the lower limit given by the trigger threshold, hence this is not an actual cut. This plot helps in finding the PSD value optimizing the n-g separation.

In order to quantify the effectiveness of the neutron-gamma discrimination, the Figure of Merit, FOM, is usually used [4]; FOM is defined as:

$$FOM = \frac{\Delta Peak}{FWHM_n + FWHM_\gamma}$$

$\Delta Peak$ = separation between the neutron and gamma peaks

$FWHM_n$ = full width at half maximum of the neutron peaks

$FWHM_\gamma$ = full width at half maximum of the gamma peaks
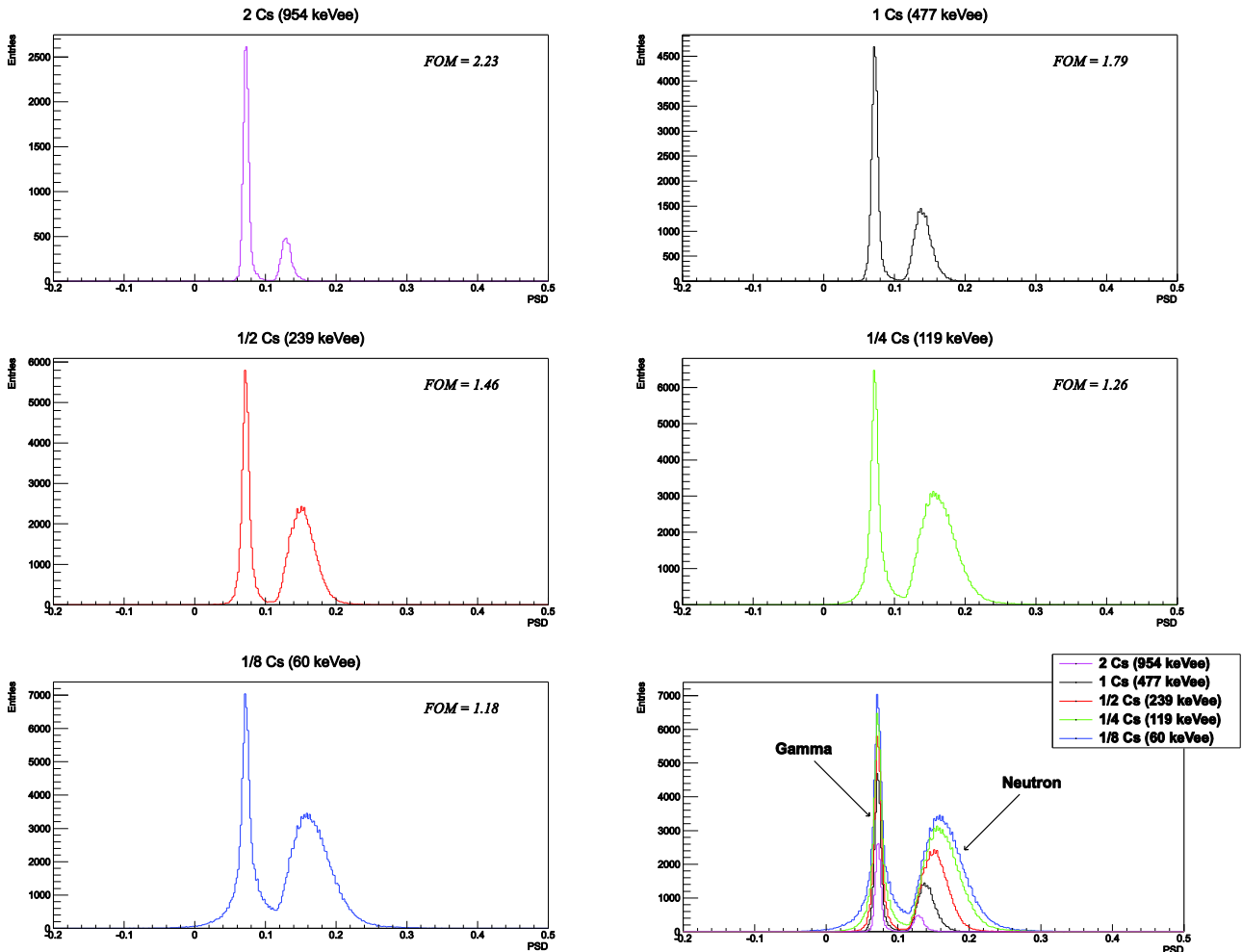
In Fig. 6 the FOM value for each energy cut is also shown.



**Fig. 6: Energy cuts with the relevant projection of Fig. 5 along the PSD axis (AmBe source @ 2 kcounts/s)**

In the final version of the DPP-PSD firmware, it will be possible to set a PSD threshold and discard all the events above it (essentially most of the gammas), since in many applications only the neutrons have to be acquired. This feature is particularly important in the cases where the counting rate of the gammas is much higher than that one of the neutrons.

Two other data acquisitions were performed increasing the count rate at 10 kcounts/s and 37 kcounts/s. In Fig. 7 and Fig. 8 the 2D plots of these acquisitions are shown.
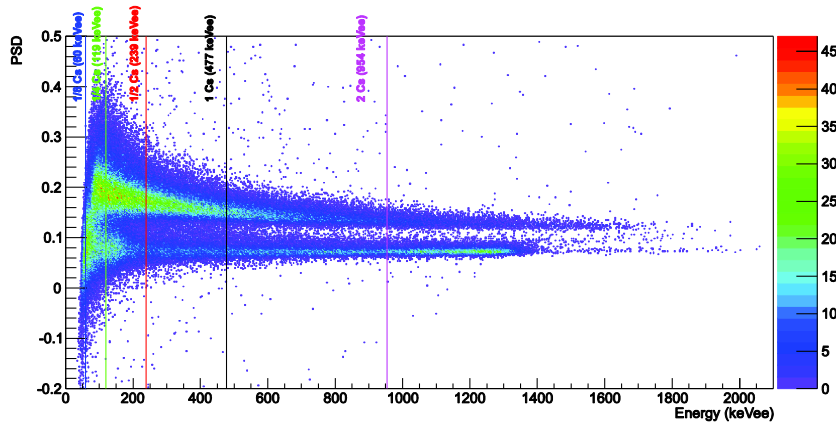
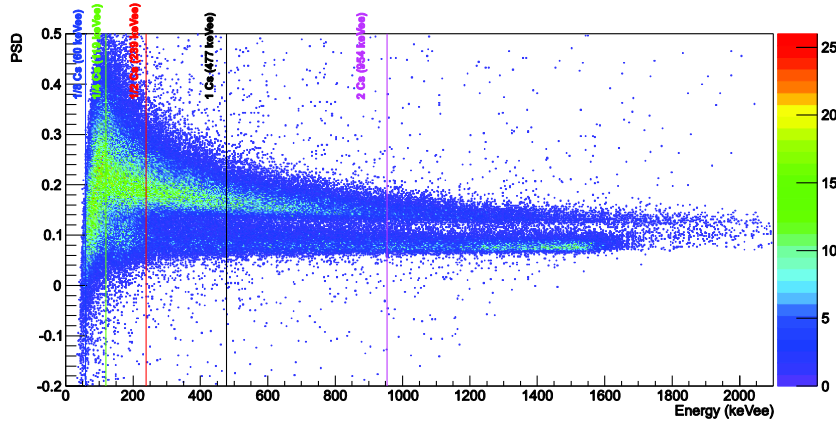**Fig. 7: 2D plot of Energy versus PSD (AmBe source @ 10 kcounts/s)**



**Fig. 8: 2D plot of Energy versus PSD (AmBe source @ 37 kcounts/s)**

Comparing the measures at 2, 10 and 37 kcounts/s we notice that, despite of a smearing of the two lobes, the neutron-gamma separation is still effective.

In Fig. 9 the projections of the 2D plots referring to the different counting rates are shown having set the energy cut to 1/4 Cs. The projections are normalized to their area in order to compare the three distributions of PSD.
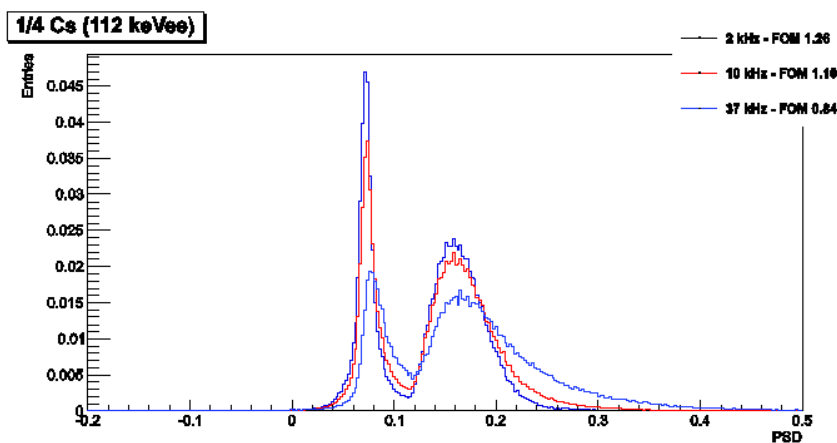


**Fig. 9: Energy cut set at 1/4 Cs with the relevant projection of the PSD axis (AmBe source @ 2 kcounts/s, 10 kcounts/s, 37 kcounts/s). The histograms are normalized to their area.)**

Considering Fig. 9, increasing the counting rate leads to two different effects in the PSD distribution: the centroids of the gamma and neutron peaks are shifted to higher values of PSD and the ratio between the gamma peak and the neutron one decreases.

The first effect is due to baseline shift caused by the tail of pulses preceding the event going to be analyzed by the DPP-PSD; vice versa, the second effect is due to pulses following the analyzed one that fall into the long gate (even partially). In this way, QL, and therefore the PSD value, increases causing a wrong identification of a large fraction of gammas as neutrons.

It is possible to modify the FPGA algorithms in order to cope with both effects: the baseline can be made more stable and precise by adding a programmable hold-off time that prevents a new trigger to open the integration gate too close to the previous pulse, thus leaving enough time for the baseline restoring. As for the multiple pulses within the gate, it is possible to implement a pile-up rejector that discards the events for which the signal presents multiple peaks. These features are currently under study.

## References

[1]    P. J. Sellin, G. Jaffar and S. D. Jastaniah, "Performance of digital algorithms for n/γ pulse shape discrimination using a liquid scintillation detector", 2003 IEEE Nuclear Science Symposium and Medical Imaging Conference Record.

[2]    W.R. Leo, "Techniques for Nuclear and Particle Physics Experiments: A How-to Approach", 2nd Revised Edition. Springer-Verlag.

[3]    G.C. Chikkura, N. Umakantha, "A new method of determining the Compton edge in liquid scintillators", *Nuclear Instruments and Methods,* Volume 107, Issue 1, 15 February 1973, Pages 201-202.

[4]    R. Aryaeinejad, J. K. Hartwell, D. F. Spencer,"Comparison between digital and analog pulse shape discrimination techniques for neutron and gamma ray separation", 2005 IEEE Nuclear Science Symposium and Medical Imaging Conference Record.

CAEN SpA
Via Vetraia 11
55049 – Viareggio Italy
Tel +39.0584.388.398
Fax +39.0584.388.959
info@caen.it   www.caen.it

www.caen.it